Material Studies in a High Energy Spark Gap

L. B. GORDON, M. KRISTIANSEN, FELLOW, IEEE, M. O. HAGLER, FELLOW, IEEE, H. C. KIRBIE, R. M. NESS, L. L. HATFIELD, AND J. N. MARX

Abstract—**The chemical interactions and physical processes occurring in a high energy spark gap with different combinations of gases, electrodes, and insulators were studied. The electrodes studied were graphite and a tungsten-copper composite; the insulators were Lexan and Blue Nylon; and the gases were N_2 and SF_6. The gas composition was monitored with a mass spectrometer. Spectroscopic techniques were used to observe the arc channel. The electrode surfaces were studied with several surface analysis techniques, including scanning electron microscopy, electron spectroscopy for chemical analysis, Auger electron spectroscopy, and X-ray fluorescence. The breakdown voltage distribution was examined for different material combinations. The plasma chemistry processes involving the gas, electrode, and insulator materials were found to affect the voltage self-breakdown distribution. The detailed surface analysis gave information about the nature of the chemical processes. The presence of Blue Nylon seemed to have a more adverse effect than Lexan and graphite seemed to have a narrower voltage distribution than the tungsten-copper composite.**

INTRODUCTION

THE PURPOSE of this study is to investigate the chemical and physical processes that lead to degradation of the electrode, gas, and insulator materials in spark gaps, and to determine how these processes vary with different combinations of the materials. Graphite or K-33 (a tungsten-copper composite) was chosen as the electrode material, Lexan or Blue Nylon as the insulator, and N_2 or SF_6 as the filler gas. These materials were chosen, based on empirical results from other work [1]-[8], as being candidates for high performance spark gap operation.

EXPERIMENTAL ARRANGEMENT

The spark gap accomodates electrodes made with inserts (5 cm in diameter and hemispherically shaped) of the various electrode materials shrunk fit into aluminum holders to obtain a tight high-current connection. A large containment cylinder (20-cm ID, aluminum) allows the electrode-gas interactions to be studied with or without an insulator adjacent to the discharge region.

The spark gap switches a simple *RC* circuit, critically damped, to give a peak current of 30 kA and a charge transfer of about 0.03 C. The gap self-breaks at 40-45 kV and switches approximately 1 kJ in 2 μs. The chamber is statically filled to 2-atm absolute pressure with the gas being studied, and is not flushed for the duration of the experimental run (10 000-50 000 shots). The gap is switched at a maximum rep-rate of two pulses per second.

Manuscript received April 20, 1982; revised July 2, 1982. This work was supported by the Air Force Office of Scientific Research.

L. B. Gordon, M. Kristiansen, M. O. Hagler, and R. M. Ness are with the Department of Electrical Engineering, Texas Technical University, Lubbock, TX 79409.

H. C. Kirbie is with the Department of Electrical Engineering, Old Dominion University, Norfolk, VA 23508.

L. L. Hatfield is with the Department of Physics, Texas Technical University, Lubbock, TX 79409.

J. N. Marx is with the Department of Chemistry, Texas Technical University, Lubbock, TX 79409.

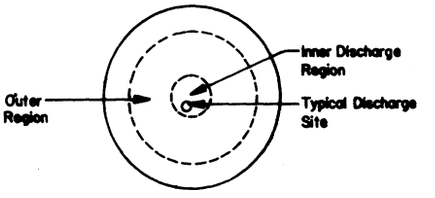

Fig. 1. Electrode discharge region boundaries.

Active on-line diagnostics used to study the gas composition and evolution and the arc channel characteristics include a mass spectrometer for gas analysis, optical spectroscopy, voltage and current measurements, and image converter and open shutter photography. Post-analysis techniques used to study the electrode and insulator surfaces and the chemical deposits removed after operation of the gap include electron spectroscopy for chemical analysis (ESCA), Auger electron spectroscopy (AES), scanning electron microscopy (SEM), X-ray fluorescence (XRF), electron microprobe analysis (EMPA), mass spectroscopy, and some analytical chemical methods.

RESULTS

In early investigations of the applicability of the surface analysis methods, brass was used as an electrode material and in the development of the gas analysis methods, air was often used as the gas [9], [10]. The investigations reported here, however, were performed with graphite and K-33 as the electrode materials, and SF_6 and N_2 as the gases.

The anode was always the electrode examined because it appeared to be the one chemically most active. Eroded samples were taken from electrodes after 50 000 shots (total charge transfer of about 1.5×10^3 C). Since 2-3 mm of electrode material is lost in the central region, initial electrode surface conditions are not critical and these electrodes were not polished. As shown in Fig. 1, samples were taken from the electrode surface in two regions. The inner discharge region is the site of all the individual discharges and had undergone erosion. The outer region is the electrode surface immediately outside the discharge region and contained chemical deposits formed by the discharge.

Surface studies were also conducted on electrodes subjected to a single shot to study the effect of one discharge on the electrode surface structure. For these studies, the electrode was polished to expose the internal matrix of the material (i.e., to get rid of machining artifacts) and then subjected to one shot.

0093-3813/82/1200-0286$00.75

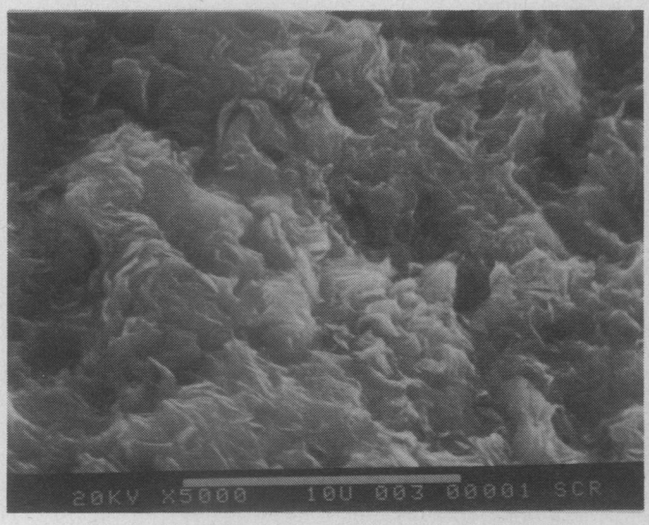

Fig. 2. Unpolished virgin graphite electrode (X 5000).

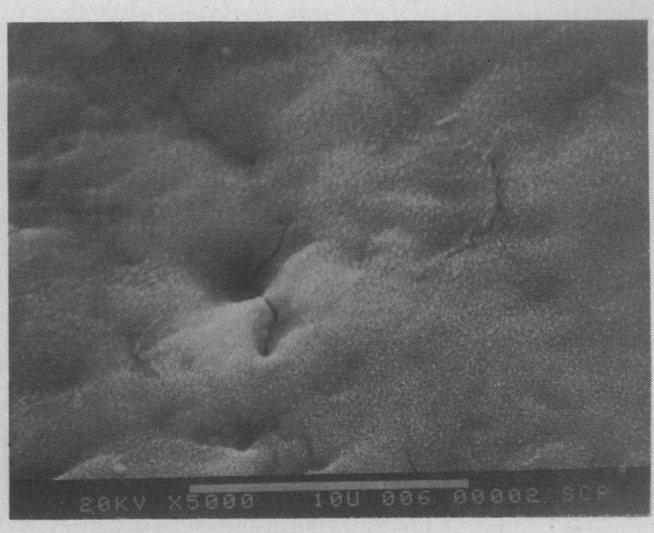

Fig. 3. Graphite electrode after 50 000 discharges in N_2 (X 5000).

All electrode samples were cut, stored, and shipped while exposed to air. Thus surface contaminants (mainly CO, CO_2, O_2, H_2O, metal oxides, and hydrocarbons) accumulate prior to surface analysis. Since ESCA and AES are both very shallow (30-80 Å) surface analysis techniques, light etching with a neutral argon beam is necessary to remove hydrocarbons, oxides, and adsorbed gases from the surface.

Graphite Electrodes

The graphite used (ACF-10Q made by Poco Graphite of Decatur, TX) is a very dense fine-grain graphite with a maximum particle size of less than 20 μm. The electrodes were made on a lathe with a steel cutting bit and show a surface structure representative of fine-grained fractured graphite (Fig. 2). No chemical agents were used and few machining marks are visible. From ESCA, the surface of the virgin electrode is 94 percent carbon and 6 percent oxygen. The oxygen is probably absorbed as O_2, CO, and CO_2 on the graphite surface. Some hydrocarbons are also invariably adsorbed on the surface but are difficult to detect on the carbon background.

After graphite electrodes were tested for 50 000 shots in N_2, the inner region of the discharge surface appeared very smooth, with extremely fine-grain structure (less than 0.1-μm particle size). Fig. 3 is an SEM of a graphite electrode exposed to 50 000 shots. The erosion process removed all traces of the original sharp fractured graphite edges, and left a smooth ablated surface. Also, the surface showed some very small (3-μm long) thermally induced cracks, and a few craters, 2-3 μm in diameter. Some graphite particles (1-10 μm in diameter) were found on insulators exposed to the graphite electrode discharge environment. From the ESCA spectrum, the virgin surface (94 percent C, 6 percent O) changed to 52 percent C, 14 percent O, and 31 percent N in the inner region, and 70 percent C, 11 percent O, and 16 percent N in the outer region after 50 000 shots. Also, a small amount of fluorine contamination (less than 2 percent) was present, due to system contamination from previous SF_6 studies.

Analysis of the gas in the N_2-graphite system by mass spectroscopy indicated an increase in CO_2 and NO_2 in the gas,

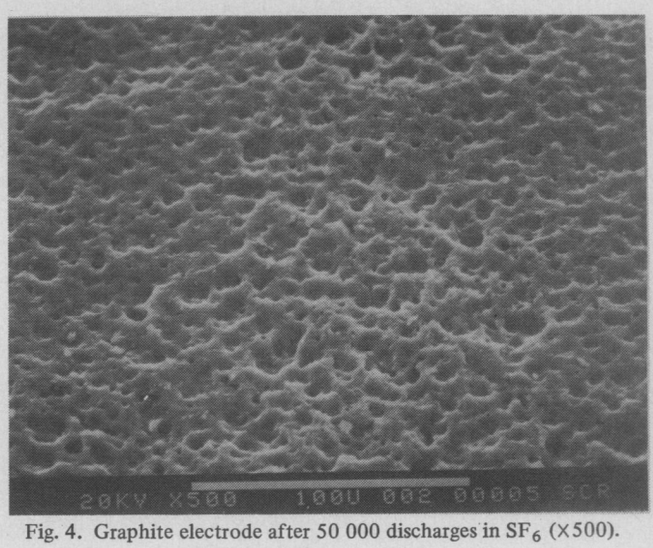

Fig. 4. Graphite electrode after 50 000 discharges in SF_6 (X500).

directly proportional to observed increases in H_2O (2-3 times higher when insulators were present, since they absorb relatively large amounts of H_2O). It was not possible to detect CO, amu 28, with the mass spectrometer, because of the presence of N_2, also amu 28. Optical spectroscopy showed an increase in the O-I line intensity after several thousand shots, indicating that the available O was indeed increasing as water was released from the surfaces.

The surface of graphite electrodes which had been fired in SF_6 (Fig. 4) showed a uniform high density of holes (craters), 5-10 μm in diameter and hemispherically shaped. Analysis of the ESCA spectrum revealed that the graphite surface contains several different carbon bonds, i.e., the broadened carbon line is composed of several components. Some of the C bonds can be identified as CF_x groups bonded on the graphite surface.

Study of the graphite surface in SF_6 is complicated by another chemical process taking place in the gap. A greyish-white powder coated everything inside the chamber, depositing a layer up to 2 mm thick on the bottom of the chamber after 50 000 shots. Chemical analysis of this powder revealed it to be primarily AlF_3, mixed with elemental aluminum and sulfur

(S_8), with traces of Al_2S_3 and absorbed gases (H_2S and SO_2). Although the chemistry is complex, the major process seems to involve fluorine atoms formed in the arc reacting with Al from the electrode holders and chamber walls to form the AlF_3. The reaction is greatly increased when aluminum vapor is ejected into the cylinder from an occasional misfire between the bottom electrode and the outer cylinder (1 in 1000 shots) or by arcing (creating more fluorine at aluminum surfaces) at electrical connections in the upper electrode holder. By ESCA the inner electrode region showed a composition of 40 percent C, 6 percent O, 32 percent AlF_3, and 20 percent CF_x groups bonded on the surface.

The outer electrode region is composed of 77 percent AlF_3, 16 percent C, and 6 percent O. The C and O most likely result primarily from surface adsorption of oxides and hydrocarbons after removal from the gap, implying that the outer region is entirely masked by deposited AlF_3, which later adsorbs the C and O. This was verified by XRF metal maps of Al on the outer region, and by scraping the deposit off to expose the virgin graphite.

Mass spectral analysis of the gas in this system is complicated by the myriad of peaks which arise from the fragmentation of SF_6 itself (SF_5, SF_4, SF_2, SF, F), although CF_4, SO_2, and H_2S could easily be detected after firing the gap. There were also detectable increases in the SF_4 and SF_2 peaks after several thousand shots. The SO_2 is probably produced by hydrolysis (reaction with H_2O) of SF_4, which is a very facile chemical reaction. Clearly, reduction and fragmentation of the SF_6 gives a multitude of products in this system.

K-33 Electrodes

The metal composite K-33 (approximately 66 percent W and 33 percent Cu), developed and manufactured by Metallwerk Plansee of Austria, and distributed by the Schwarzkopf Development Corporation in the U.S., is made by sintering tungsten powder to form a porous tungsten substrate and then infiltrating molten copper. Fig. 5 shows an SEM photograph of a polished K-33 surface. The light globular clusters are W and the filling dark material is Cu.

As with graphite, K-33 appears to undergo different chemical processes in N_2 and SF_6. In the inner region (the discharge region) in N_2, the resulting K-33 surface is very rough (Fig. 6). Analysis of the ESCA spectrum indicates a relative decrease in Cu and some increase in W in the discharge region. Very strong Cu-*I* lines are observed in the arc plasma while W was not seen.

Although the SEM photograph of the surface (Fig. 6) gives the indication of fairly deep structural changes (at least compared to graphite), a cross section of the eroded sample shows the damage to be only 3–5-μm deep, on the average, and 10-μm deep in places.

The outer region (Fig. 7) is entirely covered with vapor redeposited metal crystals. The vertical crystalline growth is in the form of dendrites, 1–4 μm in diameter and 2–8-μm tall, which are primarily composed of tungsten oxides and metallic copper. Detailed analysis of the dendrite composition is very difficult due to their small size.

After several thousand shots in SF_6, each discharge site on

Fig. 5. Polished virgin K-33 electrode (×4000).

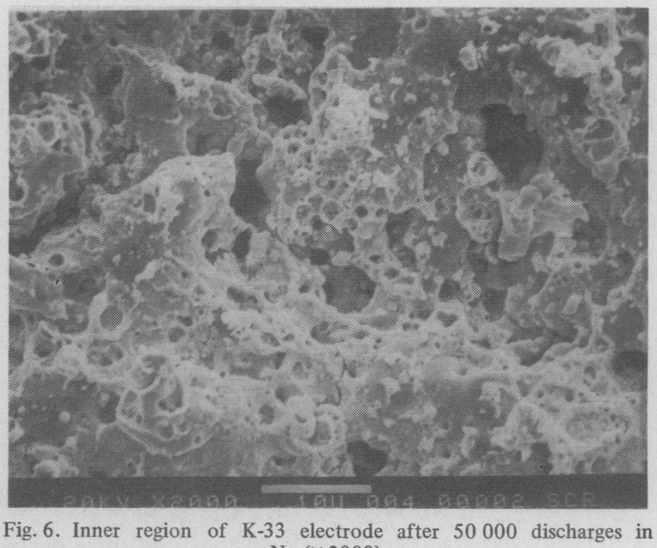

Fig. 6. Inner region of K-33 electrode after 50 000 discharges in N_2 (×2000).

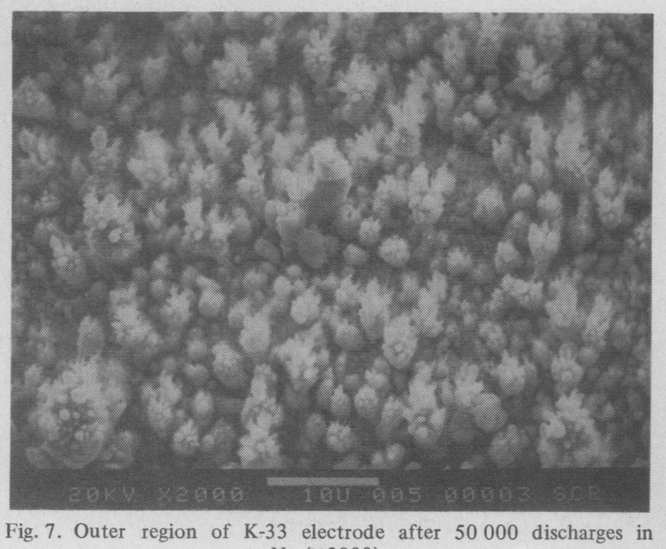

Fig. 7. Outer region of K-33 electrode after 50 000 discharges in N_2 (×2000).

Fig. 8. Center of a discharge site on a K-33 electrode after 50 000 discharges in SF_6 (X200).

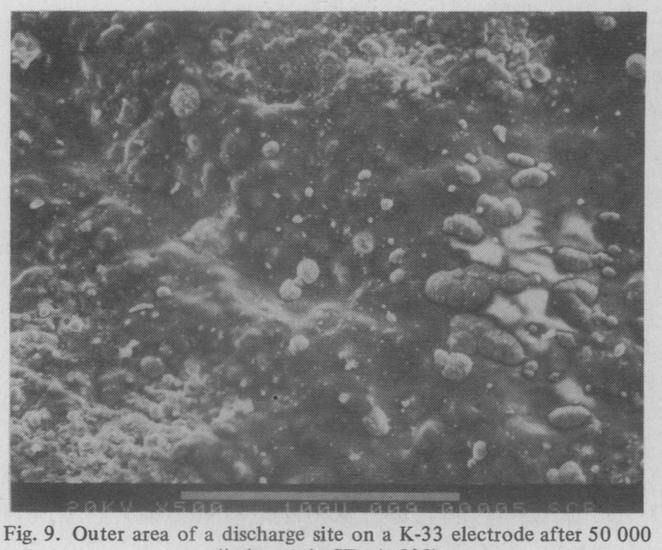

Fig. 9. Outer area of a discharge site on a K-33 electrode after 50 000 discharges in SF_6 (X500).

a K-33 electrode shows 2 distinct regions. The inner region (Fig. 8) has a regular large scale crystalline pattern, while the outer discharge site region (Fig. 9) shows a molten plastic-looking surface.

Since ESCA covers a relatively large spatial area (1 mm^2), it does not resolve the 2 regions at a single discharge site, but gives an average of the surface content. Analysis of the AES spectrum of the different areas of a single shot discharge site, however, gives very useful information concerning the effect of the single shot. Analysis of a single shot on a polished virgin surface shows 3 distinct regions. The center of a single discharge, about 1.5 mm in diameter, is a very bright dark orange star. Surrounding the center spot and filling the rest of the discharge site, about 6 mm in diameter, is a light copper-colored ring. Outside the discharge site, the polished K-33 surface is a silvery gray color (indicative of polished W). Analysis of the AES spectrum shows the virgin area to be 39 percent Cu, 14 percent W, 22 percent O, 11 percent C, 4 percent F, and 5 percent Al; the light colored ring to be 56 percent Cu, 8 percent W, 19 percent O, 7 percent C, and 6 percent F; and the dark center spot to be 63 percent CU, 0 percent W, 7 percent O, 11 percent C, and 18 percent F. The remaining components are small amounts (less than 2 percent each) of S, N, Ca, and Cl.

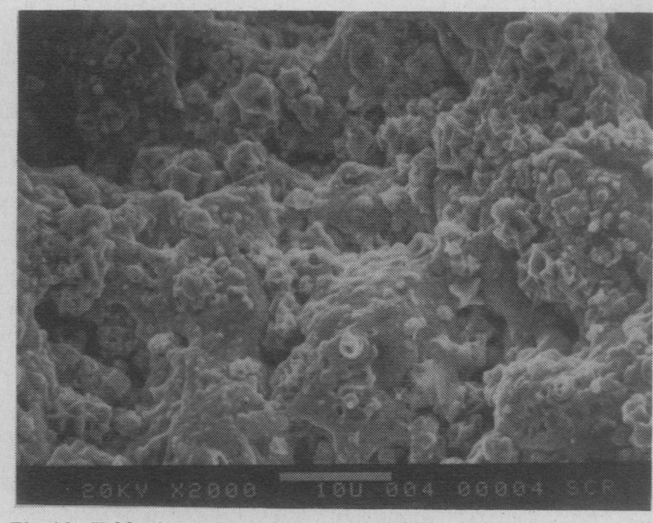

Fig. 10. K-33 electrode surface after 50 000 discharges in N_2 while exposed to lexan insulator (X 2000).

Careful analysis of the ESCA spectrum shows a very broad fluorine line (on the many-shot sample), indicating the presence of several fluorine compounds, mainly CuF_2 and fluorocarbons, and possibly CuF and CuOHF. There are two forms of carbon on the inner electrode region: the normal hydrocarbon contaminants and fluorocarbons. The carbon available for chemical reaction with F presumably comes from the normal hydrocarbon contaminants and possible impurities in the metal. Although no tungsten lines are observed in the discharge (possibly due to masking from the very strong Cu, S, and F lines), more tungsten and copper is found on insulator surfaces exposed to discharges between K-33 electrodes in SF_6 than on insulators in N_2. An accumulation of chlorine (about 5 percent) on the electrode surface is observed after 50 000 shots. Most likely the Cl is obtained as an impurity from the SF_6, which is often manufactured using Cl in the processing. Cross-section photomicrographs show the damage depth to be less than 10 μm (similar to the N_2 case).

The outer region (outside all discharges) is composed of a redeposition of material in a flake pattern characteristic of chemical deposits. It is composed of 43 percent F with less than 20-percent metal content and is very complex and difficult to analyze (from the ESCA spectrum).

Insulators

Square insulator samples (20 cm X 20 cm X 8 mm thick) were placed 5 cm from the discharge region to study the effect of the insulator presence on the electrode and the gas. Examination of the electrode surfaces exposed to insulators reveals similar characteristics, independent of the electrode material.

Fig. 10 shows a K-33 surface in N_2 exposed to Lexan. Fig. 11 is the inner region of a discharge site on K-33 in SF_6 ex-

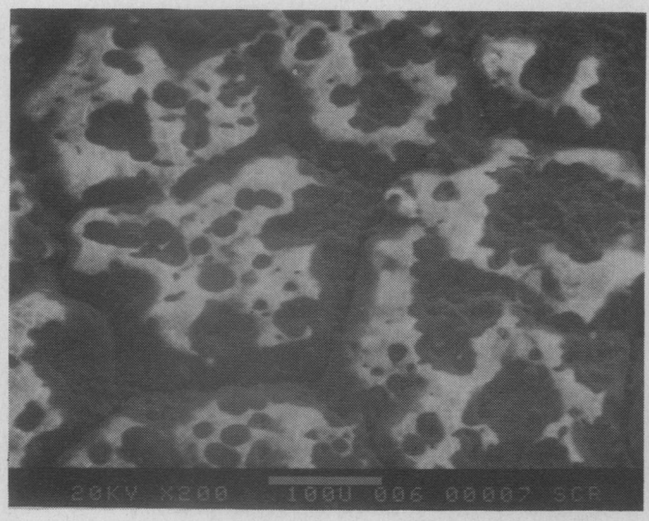

Fig. 11. Center of a discharge site on a K-33 electrode after 50 000 discharges in SF_6 while exposed to a Lexan insulator (×200).

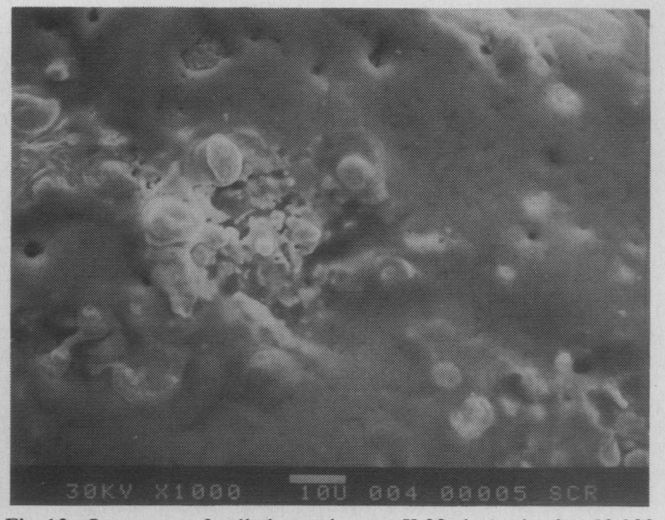

Fig. 12. Outer area of a discharge site on a K-33 electrode after 50 000 discharges in SF_6 while exposed to a Blue Nylon insulator, showing silicon nodules (×1000).

posed to Lexan. The K-33 samples are shown to illustrate the masking of the electrode surface by organic molecules. Compare, for instance, Fig. 8 with Fig. 11, and Fig. 6 with Fig. 10. Similar processes occur on graphite and brass surfaces.

Analysis of the ESCA spectrum in all cases (all combinations of electrode material and gas) when exposed to an insulator shows a high surface content of organic carbon compounds in both the inner and outer regions. An increase in H_2O is observed in N_2 when insulators are present, Blue Nylon causing the greatest increase. This is reasonable, since Lexan absorbs 3 percent water and Blue Nylon absorbs 6 percent water by weight. In an SF_6-graphite gap, an increase in CF_x compounds is observed when an insulator is present, indicating some reaction of fluorine with the insulator. Also, increases in O compounds on the electrode surfaces and in the gases (CO_2 and SO_2) are observed. In SF_6, organic fluorine compounds were found on graphite and K-33. Analysis of the ESCA spectrum shows the organic nature of the compounds, but does not indicate their exact chemical structure since the organic molecules on the electrode surface are not simple.

Three important differences are observed when Blue Nylon rather than Lexan is present in the discharge region. First, more visible deposits are observed. Second, more H_2O is released, supplying increased O for production of carbon oxides for graphite electrodes and tungsten oxides for K-33 electrodes. The third major difference is that after exposure to Blue Nylon, silicon is found on the electrode surfaces. Fig. 12 shows an SEM photograph of the outer region of a single discharge site on a K-33 electrode in SF_6. The white nodules protruding through the smooth plastic-looking deposit are some form of silicon whiskers. The smooth plastic-looking deposit surrounding the silicon nodules is a mixture of copper and copper fluorides ejected from the center of the discharge site. The silicon is observed only in the presence of Blue Nylon insulators and may come from chemicals used in the manufacture of the Blue Nylon (the mold release).

Voltage Self-Breakdown Distribution

Measurement of the voltage self-breakdown distribution has been found to be a very important diagnostic tool for spark

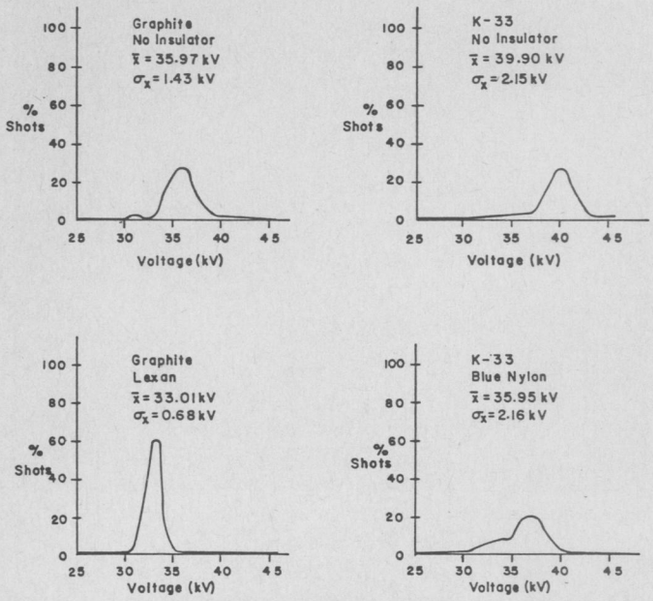

Fig. 13. Some voltage self-breakdown distribution functions after 10 000 discharges.

gaps. One seeks a distribution function that is narrow, with few or no low-voltage events. Low-voltage events imply prefires, which can be very costly in systems using a large number of spark gaps.

Fig. 13 shows some sample voltage self-breakdown distributions for the 500-shot sample window from 10 000–10 500 shots. The difference in $\bar{x}$ is primarily due to slight variations in electrode separation from case-to-case. It can be seen that the introduction of a Blue Nylon insulator in the K-33-SF_6 system leads to a significant broadening of the distribution function on the low-voltage side. On the other hand, the introduction of Lexan in a graphite-N_2 system appears to improve the distribution function. The K-33 results are consistent with the observations of the silicon nodules observed on the K-33 surface when operated in SF_6 and exposed to a Blue Nylon insulator. These nodules may lead to local field enhancement and hence prefires. The apparent improvement in

graphite N_2 data when a Lexan insulator is inserted in the gap may be due to a thick organic coating that is observed on the electrode surface in this case. This coating may serve to smooth out field enhancement points.

In work not reported here, the distribution functions have been found to undergo certain abrupt changes as the electrodes "wear themselves in" (erode). The results can therefore vary significantly depending upon how the sampling window is situated with regard to these abrupt changes. The voltage distribution results presented here should, as a consequence, be considered as qualitative. A new data acquisition system which enables continous monitoring of the breakdown voltage and its distribution function has just been installed but results are not yet available.

Discussion

Examination of the SEM photographs definitely shows different processes occurring on graphite electrodes in N_2 and SF_6. The erosion mechanism occurring in N_2 is a combination of vaporization, sublimation, and microparticle ejection. Graphite does not have a molten state at the pressures found in the gap and is mechanically stable at very high temperatures. Graphite begins to vaporize in the temperature range of 2200-2700 K, and sublimes [11] at 3640 K. The surface of the graphite electrode was apparently eroded at the point of discharge by sublimation and vaporization at surface temperatures in excess of 2500 K. Although a few craters were observed, ejection of graphite particles is probably not the major erosion mechanism since 1) the craters are too few and widely scattered to be the primary erosion process, 2) graphite vaporizes in the form of C, C_2, and C_3, and not longer chains, 3) atomic carbon is observed in the discharge (C-II lines), 4) the black deposits throughout the gap appear to be monatomic layers of amorphous carbon and not graphite particles (i.e., the deposited carbon is not polycrystalline), and 5) analysis of a single shot on a graphic electrode surface does not show pitting or craters, only preliminary smoothing. The few craters probably resulted from an occasional particle ejection or occurred at impurity sites or lattice vacancies which could be subject to accelerated chemical reactions (with O or N).

Two chemical processes were observed in the graphite-N_2 system from the ESCA results and from gas analysis. First, the change in O on the surface (after allowing for about 6 percent O adsorbed from air) is due to an increase in oxides (CO and CO_2) formed on the surface. Above 700 K, carbon oxidizes in the presence of any available oxygen and above 1000 K, carbon reacts rapidly with water. Primarily CO and CO_2 are found, depending on the relative abundance of C and O. The oxygen is obtained from the water released by all surfaces in the gap during firing, and to a lesser extent from absorbed O_2 which is also released.

The second significant chemical process occurring at the electrode is nitrogen attachment to the surface. In the inner region, N accounts for 31 percent of the surface atoms. The increases in both N and O are higher in the inner region, indicating either that the inner region (higher temperatures) is the site of more chemical activity, or that the outer region is being covered by deposited C. The increased energy spread of the ESCA carbon line on the electrode inner region (compared to the virgin sample) indicates the presence of carbon bound with another atomic species (i.e., N). Cyanogen molecules $(CN)_2$ have been spectroscopically observed by others [12] in graphite-air discharges. The exact nature of the C-N bond on the surface, or if it has any effect on erosion is not yet understood.

Graphite in SF_6 apparently undergoes a different erosion process than graphite in N_2. The uniform density and shape imply that chemical erosion is occurring at the discharge sites. Although fluorine is reacting heavily with Al to form AlF_3, it appears that some CF_x is formed on the graphite surfaces. Excess sulfur accumulates at the bottom of the gap.

The constant O-content (6 percent) in the virgin, and the inner and outer SF_6 eroded samples, is due to surface absorption after removal from the gap, implying that there was no oxygen available for reaction with the graphite surfaces, as occurred in N_2. This is consistent with observations of the gas composition showing a sharp decrease in H_2O and some increase in SO_2, and H_2S after several thousand shots. Apparently any water released in SF_6 reacts in the discharge environment before it reaches the graphite.

The K-33 electrode material in N_2 appears to undergo different processes than graphite. Unlike the chemical erosion of graphite in SF_6 or the vaporization of graphite in N_2, the K-33 appears to have undergone violent physical processes, such as melting, boiling, or spattering. The material surrounding the many pores is very similar to the appearance of the original tungsten matrix in a polished cross-section view of a virgin sample with one material depleted. Apparently the copper has been selectively boiled out or ejected from the surface. This is feasible since the melting point of copper is 1339 K and its boiling point is 2823 K, whereas W melts at 3660 K and boils at 6186 K. Thus copper boils at a temperature which is 1000 K less than that at which W melts. It is very likely that the anode spot temperature exceeds the melting and boiling points of copper. A similar process in brass [9], [10] accounts for the depletion of Zn in the discharge region and an excess of Zn immediately outside the discharge sites.

After etching, the oxygen content of the N_2 exposed K-33 electrode is significantly higher than for the virgin sample. From ESCA, it is found that all of the surface W has been oxidized, while most of the surface Cu is pure. Tungsten has a much higher reduction potential than copper and thus readily uses the oxygen released in the gap by the discharge.

The processes involved with K-33 in SF_6 are somewhat more complex than the previously described combinations. This combination is the first to show a definite effect of each individual discharge. In graphite, for instance, individual shots have no different regions and detailed analysis of the many shot surface shows no distinct pattern made by the most recent shots. In K-33, however, each of the last few shots has masked the effects of the previous shots. Two distinct regions are apparent within the inner discharge region. A single discharge (3 mm in diameter) has a center (1-2 mm in diameter) which appears to have been a molten pool of material which underwent rapid cooling from the bottom up. During cooling, recrystallization of the material produced a large scale (400 μm across) cellular pattern (Fig. 8). The pattern is most likely caused by the rapid recrystallization of CuF_2. The region immediately outside the individual discharge site (still within the inner electrode region) is composed of two materials (Fig. 9).

TABLE I
SUMMARY OF CHEMICAL RESULTS

	Property	Graphite	K-33
N_2	erosion	vaporization, sublim.	Cu boiling, W ejection
	surface texture	very smooth	rough
	outer region	nothing	Cu+W whiskers
	gas/electrode chemistry	C-N	none
	other chemistry	CO, CO_2, NO_2	WO_3 (?)
	voltage breakdown distribution	good	fair, prefires
SF_6	erosion	vap,. sub., chemical	ejection, chemical
	surface texture	smoothly pitted	crystalline (large)
	outer region	$A\ell F_3$ deposit	thick deposit
	gas/electrode chemistry	CF_x	Cu, CuF_2, WF_6 (?)
	other chemistry	S deposits, $A\ell F_3$	S deposits
	voltage breakdown distribution	fair	fair, prefires

	Lexan	Blue
H_2O content	3%	6%
contaminant	none	Si
voltage breakdown distribution	little effect	degradation

The difference in texture and form of the two materials suggests that one has a much lower melting point than the other. Possibly, one of these materials was ejected from the center of the discharge site.

A single shot on a polished K-33 electrode surface in SF_6 did not show the same pattern as a single discharge site on a multiple shot electrode. This implies that a buildup of certain chemical structure, such as CuF_2, over a period of many shots leads to the cellular structure. From the analysis of the multiple-shot sample and the single-shot sample, several important conclusions were made. First, either W is being chemically removed (by F) or the copper is being selectively drawn to the surface (at the center of the discharge site) to mask the W. Second, since there is no W exposed in the inner region, no W oxidation occurs and the 7 percent O is probably all adsorbed, whereas on the virgin region much of the 22 percent O present is in the form of oxidized tungsten. Finally, more fluorine is chemically bound to the copper in the inner region than in the virgin region.

Since some W is lost from the electrode surface, it is likely that some WF_6 is formed in the discharge plasma. No WF_6 was detected on the electrode surfaces due to its high volatility and none was seen in the filler gas because the WF_6 molecules are too heavy to detect with the mass spectrometer used. It is very likely that the electrode spot temperatures are less in SF_6 than in N_2. (Much more energy is used in dissociating the more complex SF_6 molecule.) Thus it is possible that more chemical erosion, due to fluorine, and less mechanical erosion, due to the boiling of copper, occurs in SF_6.

When comparing an electrode sample taken after 50 000 shots without an insulator with one taken after 50 000 shots with an insulator, it is apparent that the erosion mechanisms for the electrode material are basically the same (although rates may change). The electrode sample exposed to the insulator, however, is masked with organic molecules, most likely deposited after the electrode surface has cooled. The erosion details. Holes and cracks, seen previously without an insulator, are now filled and covered, although their outline can still be seen. In all cases (all combinations of K-33, graphite, N_2, and SF_6) ESCA shows a higher surface content of organic carbon compounds on the surface. Since both inner and outer areas are equally covered and since organic molecules have a low melting point (compared to the electrode materials), the material is probably deposited after each discharge.

SUMMARY

Some of the results obtained in this study are summarized in Tables I and II.

Generally, SF_6 forms chemically more active products than either air or N_2. This may be particularly important for relatively light duty gaps where chemistry may be an important part of the erosion process. In higher duty (higher Coulomb transfer per shot) gaps, the erosion process is expected to be dominated by melting and molten metal ejection. The chemistry also apparently affects the voltage self-breakdown distribution through a complicated process involving the electrode, gas, and insulator materials. The presence of Blue Nylon, which has been used in many gaps of its excellent mechanical properties, seems to affect the voltage distribution more adversely than does Lexan. Graphite, under all conditions, seems to give a narrower voltage self-breakdown distribution than K-33.

TABLE II
MATERIALS COMPARISONS

	Graphite	K-33
visual erosion	smooth	rough
erosion scale	small	large
N_2 chemistry	some (CN)	none
SF_6 chemistry	some (CF_x)	much (CuF_2, WF_6)
single discharge	little effect	much effect
V_B distribution vs no. shots	narrows	widens
cost	low	high

	N_2	SF_6
electrode chemistry	low	high
decay products	almost none	many
insulator chemistry	none	some
V_B distribution	constant	some prefires
impurities	none	Cl
expense	low	high

	Lexan	Blue Nylon
water content	low	higher
impurities	none	Si
organic contribution	some	higher
V_B distribution	little effect	higher degradation (esp. on low voltage side)

ACKNOWLEDGMENT

The authors appreciate the help of F. Williams, G. Jackson, K. Zinsmeyer, R. Curry, K. Rathbun, M. Byrd, D. Coleman, T. De La Cruz, R. Dougal, M. Foster, and J. Semrad during various phases of this work.

REFERENCES

[1] G. Marchesi and A. Maschio, "Influence of electrode materials on arc voltage waveforms in pressurized field distortion spark gaps," presented at *5th Int. Conf. Gas Discharges*, U.K., Sept. 1978.
[2] Poco Graphite–Decatur, Texas.
[3] J. E. Gruber and R. Suess, "Investigations of the erosion phenomenon in high current, high pressure gas discharges," Max Planck Inst. für Plasmaphysik, Garching, bei Munchen IPP 4/72, Dec. 1969.
[4] S. Levy, "Spark-gap erosion studies," USAELRDL Rep. 2454, Apr., 1964.
[5] F. Heitzinger, "The properties of tungsten-copper composite materials on arc erosion resistance," presented at Seminar Composite Materials in Electrotechnics, Oberursel, Germany, Oct., 1977.
[6] I. Savers, *et al.*, "Mass identified ions from spark discharge of SF_6 in the pressure range 5-67 kPa," in *Proc. IEEE Conf. Plasma Sci.*, Santa Fe, NM, May, 1981, p. 127.
[7] M. T. Buttram and G. J. Rohwein, "Operation of a 300-kV, 100-Hz, 30-kW average power pulser," in *Proc. 13th Pulsed Power Mod. Symp.*, Buffalo, NY, pp. 303-308, June, 1978.
[8] W. Hertz *et al.*, "Investigations of the properties of SF_6 as an arc quenching medium," *Proc. IEEE*, vol. 59, p. 485, 1971.
[9] L. B. Gordon *et al.*, "Investigations of the properties of a 60-kV, 5 cm spark gap for several electrode, insulator, and gas types," in *Proc. 3rd Int. Pulsed Power Conf.*, Albuquerque, NM, June, 1981, p. 376-379.
[10] L. E. Murr *et al.*, "A preliminary survey of high-energy switch materials degradation: Spectroscopic and microscopic characterization," in *Proc. 3rd Int. Pulsed Power Conf.*, Albuquerque, NM, pp. 77-80, June, 1981.
[11] M. Hatch, D. Ramakrishnan, and T. Vernardakis, "Condensation and Vaporization Coefficients of Graphite," in *Advances in Mass Spectrometry*, vol. 6, Ed., A. R. West, (Proc. conf. held in Edinburgh), p. 571-578, 1974.
[12] G. Buchet *et al.*, "CN molecular bands in a free burning metal electrode arc," *J. Phys. Collog.*, vol. 40, pp. 327-328, 1979.